High-power terahertz pulse sensor with overmoded structure*

Wang Xue-Feng(王雪锋)[a)b)], Wang Jian-Guo(王建国)[a)c)†], Wang Guang-Qiang(王光强)[a)b)], Li Shuang(李 爽)[a)b)], and Xiong Zheng-Feng(熊正锋)[a)b)]

[a)] *Northwest Institute of Nuclear Technology, Xi'an* 710024, *China*
[b)] *Science and Technology on High Power Microwave Laboratory, Xi'an* 710024, *China*
[c)] *School of Electronic and Information Engineering, Xi'an Jiaotong University, Xi'an* 710049, *China*

(Received 23 September 2013; revised manuscript received 22 October 2013; published online 25 March 2014)

Based on the hot electron effect in a semiconductor, an overmoded resistive sensor for 0.3–0.4 THz band is investigated. The distribution of electromagnetic field components, voltage standing wave ratio (VSWR), and the average electric field in the silicon block are obtained by using the three-dimensional finite-difference time-domain (FDTD) method. By adjusting several factors (such as the length, width, height and specific resistance of the silicon block) a novel sensor with optimal structural parameters that can be used as a power measurement device for high power terahertz pulse directly is proposed. The results show that the sensor has a relative sensitivity of about 0.24 kW^{-1}, with a fluctuation of relative sensitivity of no more than ±22%, and the maximum of VSWR is 2.74 for 0.3–0.4 THz band.

Keywords: hot electron effect, high power, terahertz pulse, overmoded structure

PACS: 87.50.U– **DOI:** 10.1088/1674-1056/23/5/058701

1. Introduction

The generation of high power terahertz radiation has aroused considerable interest because of its widespread applications in imaging, radar, high-data-rate communications, plasma heating and diagnostics, medical research,[1–3] etc. Vacuum electronic devices can work at room temperature, and in many publications dealing with vacuum electronic terahertz devices (such as gyrotrons, extended interaction klystrons, and various relativistic Cerenkov generators) they are extensively considered as the most promising candidates for practical applications in a frequency range of 0.1–1.0 THz.[4–6] In our research group, a 0.14-THz relativistic surface wave oscillator (RSWO) with high power output has been designed and experimented for its merits of compactness and low confined magnetic field since the year of 2007.[5,7–10] We are now working on a 0.34 THz relativistic surface wave oscillator (RSWO) with high power output.[11]

The high power terahertz wave has two main characteristics: one is a fast pulse with a duration of several nanoseconds, and the other is a high power of several megawatts.[9] Reference [8] discussed the measurement method of the frequency of the high power terahertz wave by using the subharmonic heterodyne combined with cut-off waveguide method. Here, we discuss the power measurement method.

Generally, detectors for high power narrow band terahertz pulses comprise a pyroelectric detector, Schottky diode, etc. The pyroelectric detector is capable of operating at relatively high power levels but with long response time (typically, several milliseconds). For the Schottky diode, whose response time is at about the picosecond-level, the main problem arises from the fact that it cannot handle the high power level. Hence, before being measured, the high power terahertz wave should be strongly attenuated, leading to a decrease of the measurement accuracy.

To effectively measure the power of the high power terahertz wave, a novel fundamental-mode resistive sensor (RS), based on the hot electron effect in semiconductor in high electric field,[12–15] was developed and used to detect the power generated by a high power surface wave oscillator working at 0.14 THz.[8,9,12] We are currently developing a new high power terahertz wave source working at 0.34 THz,[11] and we have designed a similar sensor by placing a silicon bar in the WR 2.8 waveguide working at the fundamental mode.[16,17] However, there are two difficulties. First, the height of the silicon bar is only 0.05 mm, and it is very difficult to realize. Second, it is very difficult to fix the sensing element in the WR 2.8 waveguide with its cross-section of 0.7112 mm×0.3556 mm. To overcome these difficulties, in this paper we propose an overmoded resistive sensor by placing the sensing element in a waveguide working at the overmoded state.

2. Physical model

2.1. Overmoded RS

A brief description of an overmoded RS is given in Fig. 1. The incident high-power terahertz pulse is received by a WR 2.8 waveguide, where the electromagnetic wave can propagate in a TE_{10} mode, it then enters into a WR 8.0 waveguide via a tapered waveguide, and interacts with a silicon block, which

*Project supported by the National Natural Science Foundation of China (Grant No. 61231003).
†Corresponding author. E-mail: wanguiuc@mail.xjtu.edu.cn
© 2014 Chinese Physical Society and IOP Publishing Ltd

is called sensing element (SE). Electromagnetic theory indicates that the electromagnetic wave can also propagate in the WR 8.0 waveguide in a TE_{10} mode for 0.3–0.4 THz band in an overmoded state.[18]

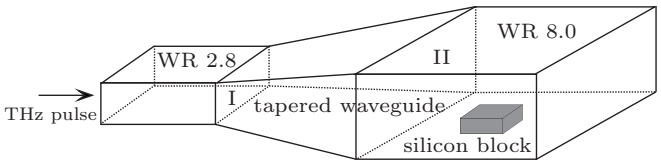


Fig. 1. Sketch of overmoded RS.

2.2. Sensing element

The high electric field of the terahertz pulse heats the electrons in a homogeneous semiconductor crystal and changes their mobility, thus increasing the resistance of the n-type silicon block fixed in the waveguide.[13–15] This is the well-known principle of the hot electrons effect and is the basis for a RS.

Figure 2 shows an *in situ* type RS model. With an n-type silicon block being fixed on the center of the wide wall of a rectangular waveguide WR 8.0, $z_{\max}$, $a = 2.032$ mm, and $b = 1.016$ mm represent the length, width, and height of the waveguide, respectively, and l, $2d$, and h denote the length, width, and height of the silicon block, respectively. The cross-section of the silicon block, serving as the sensing element of the RS, is described in Fig. 3. The silicon block is composed of the same two parts. Shortened by a metal layer on the top, one part is shortened with a wide wall of the waveguide on the bottom, while the other part is insulated from the waveguide but connected through a coaxial cable for a power supply and signal output.

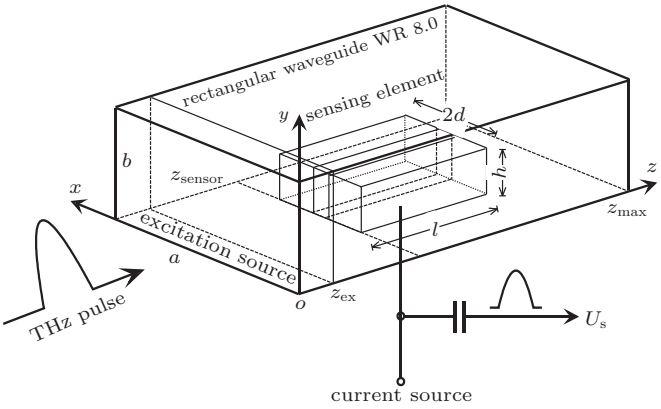


Fig. 2. *In situ* type RS.

The equivalent circuit of power measurement is shown in Fig. 2. Due to the increasing resistance of the SE, which is caused by the incident terahertz pulse, the voltage drop on the SE changes and it can be measured directly, which enables the power of the terahertz pulse to be obtained.

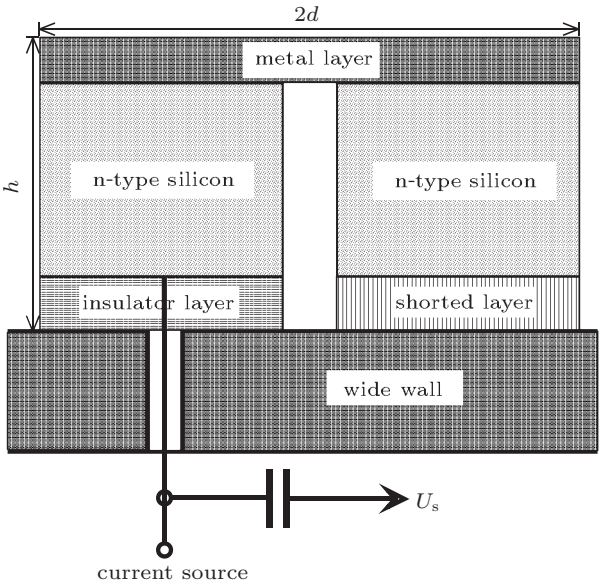


Fig. 3. Cross-section of SE.

2.3. Length of the tapered waveguide

The tapered waveguide converts the electromagnetic wave from the mode TE_{10} in the waveguide WR 2.8 into the same mode as that in the waveguide WR 8.0 as completely as possible and, hence, the transmission efficiency is one of the most important parameters. The transmission function on TE_{10} mode, which is called S_{21}, can be used as an evaluation of the transmission efficiency. The only parameter to be determined is the length of the tapered waveguide in Fig. 1. The amplitudes of S_{21} for four different lengths are calculated by using the finite-difference time-domain (FDTD) method[19], which are shown in Fig. 4 in a frequency band of 0.3–0.4 THz. It can be seen from Fig. 4 that the amplitudes of S_{21} are all greater than 0.96 and the 25 mm-length is rather less fluctuated.

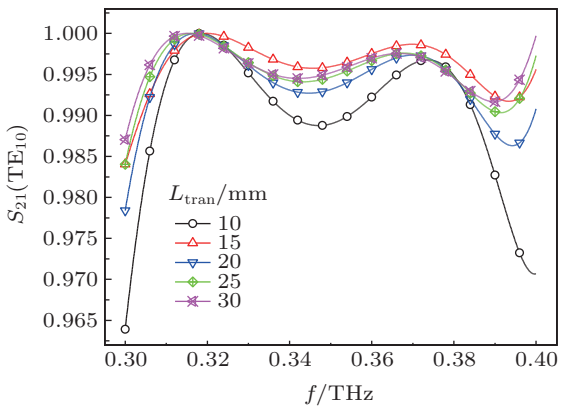


Fig. 4. (color online) Variations of the amplitudes of S_{21} with frequency in a band of 0.3–0.4 THz.

3. Distribution of the electric field

A three-dimensional (3D) FDTD method is used to simulate the field distribution within the model, as shown in Fig. 2. For the TE_{10} mode, $E_x = H_y = E_z = 0$, H_x, E_y, and H_z can all be excited in analytic form according to microwave theory. The convolutional perfectly matched layers (CPMLs)[20] are set to be in planes $z = 0$ and $z = z_{max}$. A maximum electromagnetic wave reflection coefficient of no more than 10^{-3} is achieved. The 3D FDTD method can be used to simulate the interactions between high-power terahertz pulse and the n-type silicon block.

Figure 5 shows the distribution of E_y during the interaction within waveguide WR 8.0 (frequency 0.34 THz, $z_{max} =$ 3 mm, plane $y = h/2$, $\rho = 1$ Ω·cm, and the relative dielectric constant of the n-type silicon block is $\varepsilon = 11.9$). As a result of the insertion of the silicon block, more perturbations occur in the E_y-distribution. As is well know, the amplitude of E_y for mode TE_{10} can be expressed as $|E_y| = E_0 \sin(\pi x/a)$, and it reaches a maximum in the center of the wide wall ($x = a/2$) and a minimum on the edge of the wide wall ($x = 0$ and $x = a$) in an empty rectangular waveguide. Because the scattering and absorption are caused by the sensing element, a standing-wave occurs and obvious attenuation of $|E_y|$ takes place. In addition, it is obvious that the unsymmetry of excitation source in the z-direction in Fig. 2 leads to the unsymmetric distribution of $|E_y|$ in the same direction in Fig. 5.

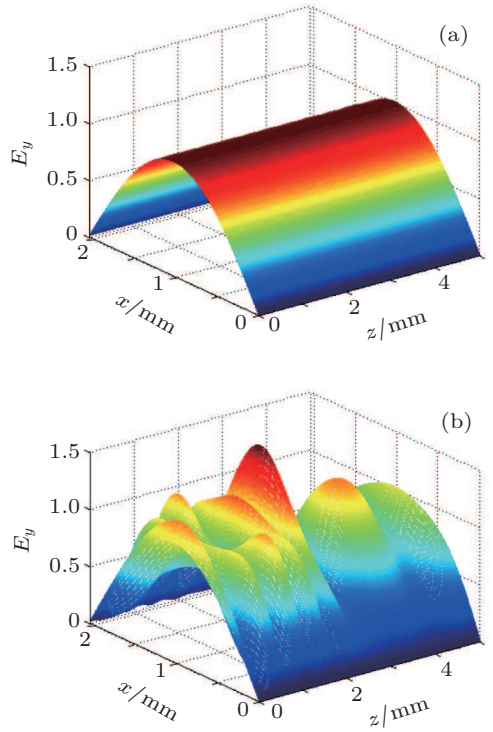


Fig. 5. (color online) Distributions of E_y in (a) empty waveguide and (b) waveguide with SE, with $l = 0.65$ mm, $2d = 0.6$ mm, $h = 0.2$ mm, $\rho = 2$ Ω·cm, $f = 0.34$ THz, $z_{max} = 5$ mm, and plane $y = h/2$.

4. Parameters of the sensing element

4.1. Voltage standing wave ratio (VSWR)

Figure 6 shows the dependences of VSWR on the length, width, height and specific resistance of a silicon block. It can be seen from Fig. 6 that h is the most important factor to VSWR, $2d$ and ρ both have effects on VSWR to some extent, and l influences the frequency which the extremum value of the VSWR reaches. In fact, the reason why h and $2d$ have

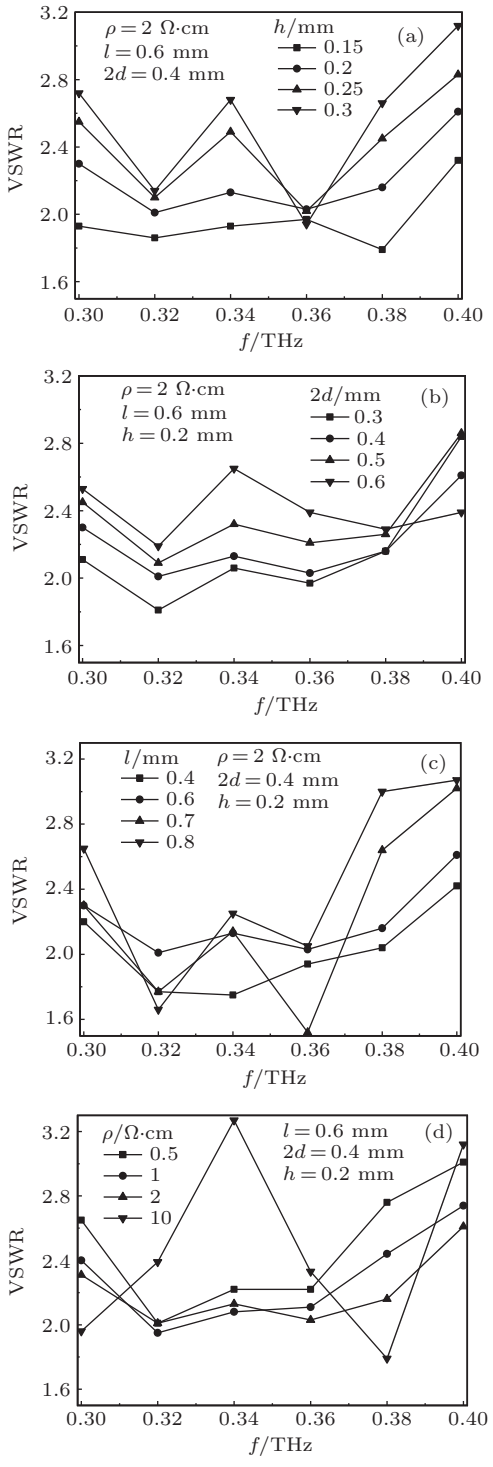


Fig. 6. Dependences of VSWR on frequency at different values of the height (a) length (b), width (c), and specific resistance (d) of a silicon block.

effects on VSWR is mainly that the increase of $2d$ (or h) would increase the area of the cross section of a sensing element, thereby leading to an increase of VSWR.

In summary, l, $2d$, h, and ρ can all influence VSWR to some extent and h is the most important. In the case of $h = 0.2$ mm in which VSWR can be kept lower for 0.3–0.4 THz band, a possible optimal height of the RS is determined.

4.2. Optimization of relative sensitivity

According to the hot electron effect, the relative difference in resistance of the sensing element, $\Delta R/R$, is proportional to the power of the electromagnetic wave that propagates in the waveguide, thus the relative sensitivity of an RS can be defined as

$$\xi = \frac{\Delta R/R}{P}, \tag{1}$$

and the relative difference in resistance of the sensing element can be expressed as

$$\frac{\Delta R}{R} = \beta \left[\frac{1}{2} + \frac{1}{1+(2\pi f \tau_\varepsilon)^2}\right] \langle E^2 \rangle, \tag{2}$$

where f is the frequency of electric field, β is the hot-electron coefficient in a DC electric field, τ_ε is the energy relaxation time of hot electron, and $\langle E^2 \rangle$ is the average value of the square of the electric field within sensing element. Let P be the level of power that propagates through the waveguide, E_0 which is the maximum of electric field amplitude of the TE_{10} mode in a rectangular waveguide can be expressed as

$$P = \frac{abE_0^2}{480\pi}\sqrt{1-(c/2af)^2}. \tag{3}$$

As it is overmoded transmission that the electromagnetic field in TE_{10} mode at frequencies from 0.3 THz to 0.4 THz passes through waveguide WR 8.0, the relative sensitivity of an *in situ* RS can be written as[16]

$$\xi(f) = \frac{480\beta\pi}{ab\sqrt{1-(c/2af)^2}} \left[\frac{1}{2} + \frac{1}{1+(2\pi f\tau_\varepsilon)^2}\right] \frac{\langle E^2 \rangle}{E_0^2}, \tag{4}$$

where c is the speed of light in free space.

For a real application, the relative sensitivity of an ideal RS should be kept constant in a 0.3–0.4 THz band. Let f_1 be the lowest interested frequency, and assume $\xi(f)$ to be kept unchanged for $f > f_1$ in the 0.3–0.4 THz band, in other words, $\xi(f) \equiv \xi(f_1)$. According to Eq. (4), two dimensionless parameters, $\eta_{\text{ideal}}(f)$ and $\eta_{\text{cal}}(f)$, can be defined as

$$\eta_{\text{ideal}}(f) = \left[\frac{1+2/[1+(2\pi f_1\tau_\varepsilon)^2]}{1+2/[1+(2\pi f\tau_\varepsilon)^2]} \sqrt{\frac{1-(\lambda/\lambda_c)^2}{1-(\lambda_1/\lambda_c)^2}}\right]^{\frac{1}{2}}, \tag{5}$$

$$\eta_{\text{cal}}(f) = \left[\frac{\langle E^2(f)\rangle/E_0^2(f)}{\langle E^2(f_1)\rangle/E_0^2(f_1)}\right]^{\frac{1}{2}}, \tag{6}$$

where λ and λ_c represent the wavelength of electric field and cutoff wavelength of the waveguide, respectively. It is obvious that $\eta_{\text{ideal}}(f) \equiv \eta_{\text{cal}}(f)$ only if $\xi(f)$ is kept constant in the range of 0.3–0.4 THz; that is to say, equations (5) and (6) can be used for the optimization of relative sensitivity of an RS. By comparing $\eta_{\text{ideal}}(f)$ with $\eta_{\text{cal}}(f)$, one can easily obtain a series of parameters of an optimal RS, including l, $2d$, and ρ.

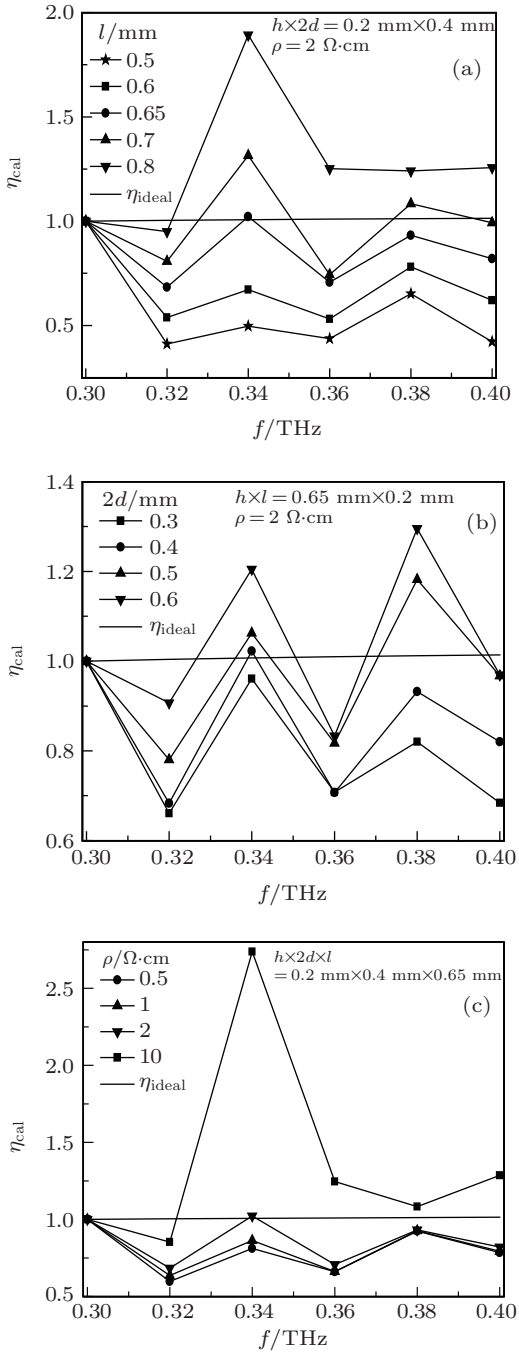


Fig. 7. Dependences of η_{cal} on length (a), width (b), and specific resistance (c) of a silicon block.

The dependences of η_{cal} on l, $2d$, and ρ of the silicon block in the 0.3–0.4 THz frequency band are shown in Fig. 7. Some conclusions can be made from this figure. First, being contrary to the long-l case, η_{cal} decreases at lower frequencies

while it increases at higher frequencies in short-l case, and $l = 0.65$ mm may be a good optimal solution in comparison of $\eta_{\rm cal}$ with $\eta_{\rm ideal}$. Second, $2d$ can also influence $\eta_{\rm cal}$ to some extent, $2d = 0.6$ mm is in better agreement with the case of $\eta_{\rm ideal}$ than all of the four cases. Third, ρ affects $\eta_{\rm cal}$ greatly. The larger the value of ρ is, the larger the deviations of $\eta_{\rm cal}$ and $\eta_{\rm ideal}$ are. It can also be seen from Fig. 7 that $\eta_{\rm cal}$ accord better with $\eta_{\rm ideal}$ than in the case $\rho = 2\ \Omega$·cm.

Four parameters (i.e., the height, width, length, and specific resistance of the silicon block) have all been determined and, as a result, the overmoded RS is put forward, which proceeds from a larger size of cross-section than that of the single mode one, and shows that it is perfectly feasible to complete. The relative sensitivity and VSWR of the overmoded RS are shown in Fig. 8. It can be inferred from Fig. 8 that the relative sensitivity is about 0.24 kW^{-1}, the fluctuation of its relative sensitivity is no more than ±22%, and the maximum of VSWR is 2.74 in the 0.3–0.4 THz band.

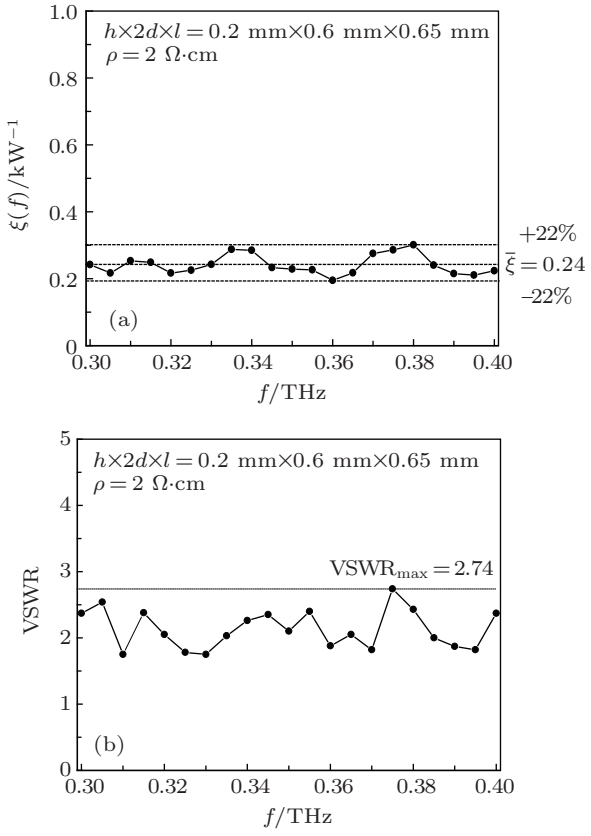


Fig. 8. Relative sensitivity (a) and VSWR (b) versus frequency of the sensor.

According to dependence of the transmission power on VSWR and voltage reflectance Γ, let VSWR = 2.74, then $\Gamma = 0.45$, the power reflectance would be 0.2. That is to say, the relative error of measurement would be no more than 20%.

5. Conclusions

An overmoded RS for the 0.3–0.4 THz band is investigated in this paper, and a novel RS that can be directly utilized for high-power terahertz pulses measurement is presented. The structure consists of a window of waveguide WR 2.8, a section of tapered waveguide whose length is 25 mm, and a window of waveguide WR 8.0. Distributions of electric field components and VSWR within the waveguide WR 8.0, and average electric field in the silicon block are discussed. The relative sensitivity of RS is about 0.24 kW^{-1}, with a fluctuation range of no more than ±22%, and its VSWR is less than 2.74 in the 0.3–0.4 THz frequency band. Owing to the larger size of the cross-section of the waveguide window and the thicker sensing element, the RS is shown to be perfectly feasible to be produced.

References

[1] Siegel P H 2002 *IEEE Transaction on Microwave Theory and Techniques* **50** 910
[2] Booske J, Dobbs R, Joye C, Kory C, Neil G, Park G, Park J and Temkin R 2011 *IEEE Transaction on Terahertz Science and Technology* **1** 54
[3] Chen Z and Cao J C 2013 *Chin. Phys. B* **22** 059201
[4] Li Y T, Wang W M, Li C and Sheng Z M 2012 *Chin. Phys. B* **21** 095203
[5] Zhang H, Wang J G, Tong C J, Li X Z and Wang G Q 2009 *Phys. Plasmas* **16** 123104
[6] Xu X, Wei Y Y, Shen F, Huang M Z, Tang T, Duan Z Y and Gong Y B 2012 *Chin. Phys. B* **21** 068402
[7] Li X Z, Wang J G, Song Z M, Chen C H, Sun J, Zhang X W and Zhang Y C 2012 *Phys. Plasmas* **19** 083111
[8] Wang G Q, Wang J G, Li X Z, Fan R Y, Wang X Z, Wang X F and Tong C J 2010 *Acta Phys. Sin.* **59** 8459 (in Chinese)
[9] Wang G Q, Wang J G, Tong C J, Li X Z, Wang X F, Li S and Lu X C 2013 *Phys. Plasmas* **20** 043105
[10] Wang G Q, Wang J G, Li S, Wang X F, Tong C J, Lu X C and Guo W J 2013 *Acta Phys. Sin.* **62** 150701 (in Chinese)
[11] Li S, Wang J G, Tong C J, Wang G Q, Lu X C and Wang X F 2013 *Acta Phys. Sin.* **62** 120703 (in Chinese)
[12] Wang G Q, Wang J G, Tong C J, Li X Z and Wang X F 2011 *Acta Phys. Sin.* **60** 030702 (in Chinese)
[13] Liu E K, Zhu B S and Luo J S 2011 *The Physics of Semiconductors* (7th edn.) (Beijing: Publishing House of Electronics Industry) pp. 116–121 (in Chinese)
[14] Dagys M, Kancleris Ž, Simniškis R, Schamiloglu E and Agee F J 2001 *IEEE Antennas and Propagation Magazine* **43** 64
[15] Kancleris Ž, Simniškis R, Dagys M and Tamošiūnas V 2007 *IET Microw. Antennas Propag.* **1** 757
[16] Wang X F, Wang J G, Wang G Q, Tong C J, Li S and Li Y 2013 *High Power Laser and Particle Beams* **25** 455 (in Chinese)
[17] Wang X F, Wang J G, Wang G Q, Wang W, Zhu X Q and Li S 2013 *Cross Strait Quad-Regional Radio Science and Wireless Technology Conference*, July 21–25, 2013, Chengdu, China, p. 413
[18] Zhang K Q and Li D J 2002 *Electromagnetic Theory for Microwaves and Optoelectronics* (2nd edn.) (Beijing: Publishing House of Electronics Industry) pp. 239–241 (in Chinese)
[19] Ge D B and Yan Y B 2006 *Finite-Difference Time-Domain Method for Electromagnetic Waves* (2nd edn.) (Xi'an: Xidian University Press) p. 12 (in Chinese)
[20] Wang Y, Wang J G and Zhang D H 2005 *High Power Laser and Particle Beams* **17** 1557 (in Chinese)